

Dispersion cancellation in a quantum interferometer with independent single photons

DONG-GIL IM, YOSEP KIM,  AND YOON-HO KIM* 

Department of Physics, Pohang University of Science and Technology (POSTECH), Pohang 37673, Republic of Korea

*yooho72@gmail.com

Abstract: A key technique to perform proper quantum information processing is to get a high visibility quantum interference between independent single photons. One of the crucial elements that affects the quantum interference is a group velocity dispersion that occurs when single photons pass through a dispersive medium. We theoretically and experimentally demonstrate that an effect of group velocity dispersion on the two-photon interference can be cancelled if two independent single photons experience the same amount of pulse broadening. This dispersion cancellation effect can be applied to a multi-path linear interferometer with multiple independent single photons. As multi-path quantum interferometers are at the heart of quantum communication, photonic quantum computing, and boson sampling applications, our work should find wide applicability in quantum information science.

© 2021 Optical Society of America under the terms of the [OSA Open Access Publishing Agreement](#)

1. Introduction

Quantum interference effects are at the heart of various quantum information processing applications, including quantum communication [1,2], quantum teleportation [3–6], quantum imaging [7–10], quantum metrology [11], and quantum computing [12,13]. Therefore, in photonic quantum information, attaining high visibility quantum interference is often synonymous to demonstrating the desired quantum information tasks. One of the crucial elements that affects the quantum interference is the group velocity dispersion that occurs when the single photons pass through a dispersive medium [14–20]. Such dispersive medium can be an optical fiber to transport the single photons [21] and other optical components in the interferometer. Especially, if the photon bandwidth is large, even for a thin medium, the dispersion effects should be considered and dealt with properly.

One of the simplest systems for the quantum interferometer is the two-photon interferometer [22] in which two indistinguishable single photons injected into each input mode of a 50/50 beam splitter become coalesced and found together in either one of the two output modes of the beam splitter due to the bosonic nature of photons. The dispersion effect on the two-photon interference with photon pairs generated via spontaneous parametric down-conversion (SPDC) process has been extensively studied for the fundamental aspects [23–27] and shown that a dispersive medium in one arm does not affect the two-photon interference if there is frequency anti-correlation between two entangled-photons. This effect of dispersion cancellation based on frequency anti-correlation between the entangled photons has been applied to particular applications such as quantum optical coherence tomography [28,29] and quantum clock synchronization [30]. It is worthwhile to note that frequency anti-correlation between the entangled photons also allows non-local dispersion cancellation in which the two or more photons never interact with each other at a beam splitter before detection [31–33].

For quantum information processing applications, however, quantum interference with the independent single photons [34] has broader applicability and, therefore, it is necessary to understand how to deal with the negative effects of dispersion in this scenario. In particular, an

interesting question arises as to whether it would be possible to achieve dispersion cancellation in a multi-mode quantum interferometer with independent single photons, see Fig. 1.

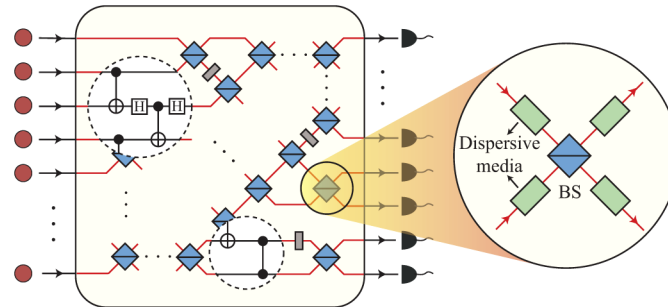


Fig. 1. Schematic of a photonic quantum computing circuit. Linear optics are used for implementing quantum gates and all such optical elements introduce dispersion to the single photon pulses.

In this paper, we theoretically and experimentally demonstrate that the effect of group velocity dispersion in a quantum interferometer can be cancelled even with independent single photons at the input. Specifically, we show that Hong-Ou-Mandel-type two-photon interference with independent single photons at the input to the beam splitter exhibits cancellation of the group velocity dispersion effect if two independent single photons experience the same amount of pulse broadening before injected into a beam splitter. Each single photon pulse, prepared by heralding a photon of the photon pair born in the process of SPDC pumped by a femtosecond pulsed laser, becomes broadened as a result of propagation through a single-mode optical fiber [35]. However, the two-photon interference does not exhibit any broadening, thereby exhibiting cancellation of group velocity dispersion in a quantum interferometer if the independent single photon pulse experiences the same amount of dispersion before the beam splitter. Moreover, our theoretical analyses show that this dispersion cancellation effect can be applied to multi-path linear interferometer with multiple independent single photons which is used to implement a unitary transformation on single photons for the purpose of realizing quantum gates [36,37] for photonic quantum computation [12,13,38,39] and experimental boson sampling [40–42].

2. Experiment

The experimental setup is schematically shown in Fig. 2(a). Femtosecond laser pulses (80 MHz, 780 nm, temporal duration 140 fs) from a Ti:sapphire oscillator are frequency doubled and pump two 1-mm-thick type-II BBO crystals for the SPDC process. The non-collinear degenerate SPDC photons have the center wavelength of 780 nm and the heralding photons are detected at the detectors D_1 and D_2 after passing through 10 nm full width at half maximum (FWHM) bandpass filters (BF). The two independent heralded single photons pass through the single-mode optical fibers having the same group velocity dispersion β and lengths of L_1 and L_2 . The single photons are then injected into the two input ports of a 50/50 beam splitter for the Hong-Ou-Mandel type two-photon interference measurement. Finally, heralded single photons are detected at the detectors D_3 and D_4 after passing through BFs. We observed the two-photon interference pattern between the two heralded single photons by monitoring the four-fold coincidence count rates as a function of the relative optical time delay τ in the two arms.

Since we make use of type-II SPDC for the photon pair generation, the signal and idler photons of SPDC have a specific frequency correlation or joint spectral intensity (JSI) as shown in Fig. 2(b). So, the 10 nm FWHM BFs placed in front of the heralding detectors D_1 and D_2 will cause tracing out of the idler photon spectral modes, resulting in spectrally mixed heralded single

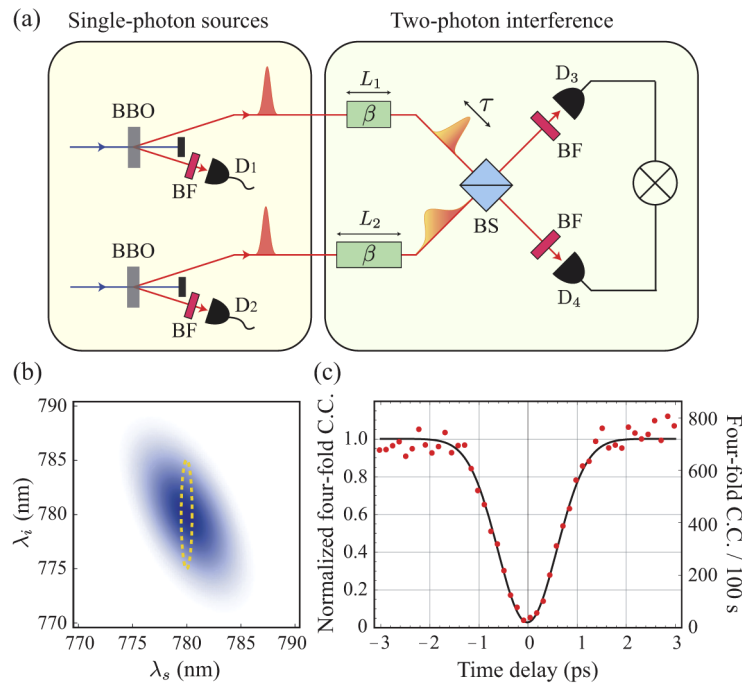


Fig. 2. (a) Schematic of the experiment. Two independent heralded single photons are prepared via the SPDC process and sent to a beam splitter (BS) after passing through the optical fibers of lengths L_1 and L_2 . The group velocity dispersion of the optical fiber is β . (b) Calculated joint spectral intensity (JSI) of the SPDC photon pair. The yellow dashed ellipse represents the JSI when the heralded single photons are filtered by 1 nm FWHM bandpass filters (BF) while the heralding photons are filtered by 10 nm FWHM BFs. (c) With the heralded single photon bandwidth set at 1 nm FWHM, even with $L_1 = L_2 = 6$ m, we observe high visibility quantum interference of 97%. This is due to the fact that single photons of 1 nm bandwidth do not produce significant pulse broadening. For (c), the average pump power of 150 mW is used and the average background noise counts coming from the multiple pairs of SPDC photons is 251 for accumulation time of 100 s. The solid circles are the normalized four-fold coincidence count rates and the solid line represents Gaussian fits to the data points.

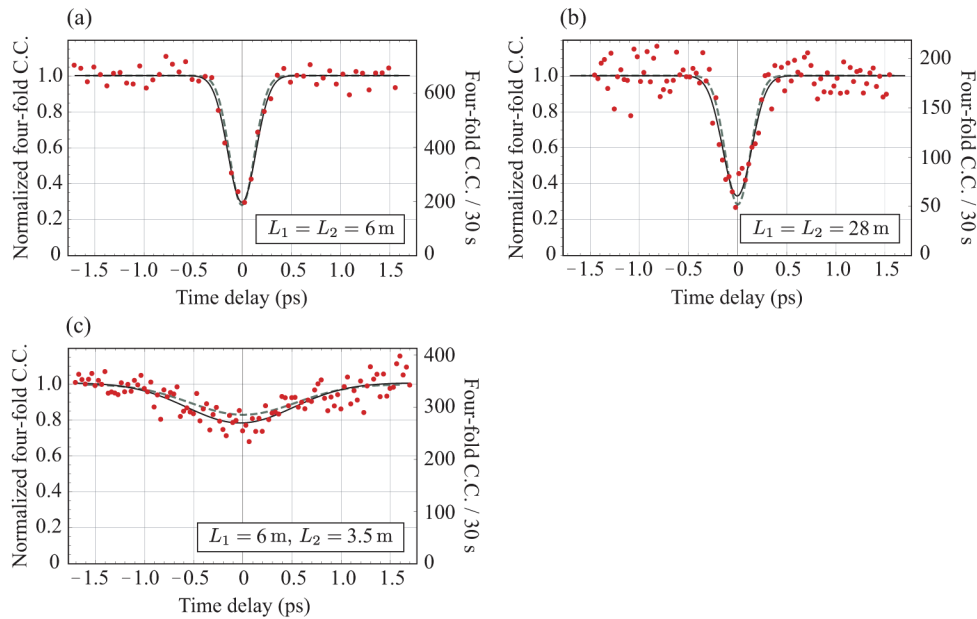


Fig. 3. Experimental results confirming dispersion cancellation in a two-photon quantum interferometer with independent heralded single photons. The bandwidths of the heralded single photons are set at 10 nm. (a) When the optical fibers are of the same lengths, $L_1 = L_2 = 6$ m, the group dispersion effects to the single photon is not observed in the two-photon quantum interference. (b) Even when the optical fiber lengths are increased to $L_1 = L_2 = 28$ m, two-photon quantum interference do not exhibit the group velocity dispersion effects. (c) When the lengths are different, $L_1 = 6$ m, $L_2 = 3.5$ m, the group velocity dispersion effects are clearly seen with the broadening of the two-photon interference dip and reduction of the visibility. The solid circles are the normalized four-fold coincidence count rates and the solid lines represent Gaussian fits to the data points. The average pump power of 50 mW is used for these experiments and the average background noise counts coming from the multiple pairs of SPDC photons are (a) 76, (b) 21, and (c) 50 for accumulation time of 30 s. The dashed lines show the results of the theoretical calculation of the two-photon interference.

photon states for the signal photons. First, to ensure that the experimental setup is properly aligned, the BFs in front of the detectors D_3 and D_4 are set at 1 nm FWHM. The yellow dashed ellipse in Fig. 2(b) represents the JSI when the heralded single photons are filtered by 1 nm FWHM BFs while the heralding photons are filtered by 10 nm FWHM BFs. It is clear that the filtering process has removed frequency correlation between the signal and idler photons, allowing us to prepare spectrally pure heralded single-photon states. Then, with the lengths of the optical fibers set at $L_1 = L_2 = 6$ m, we observe the four-fold coincidence count rates as a function of the optical delay τ . The results of this experiment is shown in Fig. 2(c). With the heralded single photon bandwidth set at 1 nm FWHM, even with $L_1 = L_2 = 6$ m, we observe high visibility quantum interference of 97%. This is due to the fact that single photons of 1 nm bandwidth do not produce significant pulse broadening. In order to estimate the background noise counts coming from the multiple pairs of SPDC photons which will lead to the erroneous heralding rates, we additionally measured the four-fold coincidence count rates by blocking one of the SPDC sources and then by blocking the other SPDC source.

To add noticeable dispersion effects to the heralded single photons for the optical fiber used in the experiment, it is necessary for us to change the lengths (L_1 and L_2) and the bandwidths of

the single photons. Note that, for the fused silica core of the optical fiber, the group velocity dispersion parameter β at 780 nm is $37.802 \text{ fs}^2/\text{mm}$. First, the bandwidths of the heralded single photons are changed to 10 nm by using 10 nm FWHM BFs in front of detectors D_3 and D_4 . Then the two-photon interference measurement is carried out by interfering two independent single photons by passing them through optical fibers of different lengths (L_1 and L_2).

The experimental results confirming dispersion cancellation in a quantum interferometer with independent heralded single photons are shown in Fig. 3. First, the lengths of the optical fibers are set at $L_1 = L_2 = 6 \text{ m}$. In this condition, the 10 nm bandwidth single photon pulse is expected to be broadened to 9.84 ps in time. However, the data in Fig. 3(a) show clearly that the group velocity dispersion effect has been cancelled out: the FWHM width of the two-photon interference dip is 0.34 ps, significantly smaller than the expected pulse broadening. The two-photon visibility is 70.4% in Fig. 3(a) which is smaller than that of Fig. 2(c), but this is unrelated to the group velocity dispersion effect. Rather, the reduced visibility is attributed to the frequency correlation nature of SPDC photons used in the experiment. While the increased single photon bandwidths of 10 nm do provide large enough bandwidths for noticeable pulse broadening, it also introduces unwanted spectral correlation between the heralding and the heralded photons, causing reduction of two-photon interference visibility [43,44]. Second, the lengths of the optical fibers are now set at $L_1 = L_2 = 28 \text{ m}$ and, in this condition, the 10 nm bandwidth single photon pulse is expected to be broadened to 45.9 ps in time. However, the experimental data shown in Fig. 3(b) clearly demonstrate that the dispersion effect has been cancelled out: the FWHM width of the two-photon interference dip is 0.35 ps, similarly to Fig. 3(a). The two-photon interference visibility is slightly reduced to 67.4% from 70.4% of Fig. 3(a) for the same reason mentioned above. Finally, when the lengths of the optical fibers are different, $L_1 = 6 \text{ m}$, $L_2 = 3.5 \text{ m}$, the effects of dispersion show up immediately, see Fig. 3(c): the FWHM width of the two-photon interference dip is broadened to 1.28 ps and the visibility has been significantly lowered to 22.9%. Note that for the case of $L_1 = 6 \text{ m}$, $L_2 = 3.5 \text{ m}$, the optical fiber length difference between the two arms is compensated by the additional free space path so that the single photons from the both arms arrive simultaneously at the beam splitter.

The experimental results in Fig. 3 make it clear that, when two independent single photons experience different amount of dispersion, the effects of dispersion appear at two-photon quantum interference. However, when the two photons experience the same amount of dispersion, the dispersion effect is cancelled out completely, exhibiting the same two-photon interference feature as if there had been no dispersion induced pulse broadening.

3. Theory

3.1. Dispersion cancellation with two independent single photons

In order to describe the dispersion cancellation effect on the two-photon interference theoretically, we begin our study by writing the SPDC two-photon state in the Schmidt decomposed form which is useful for describing the heralded single photon state [43],

$$\begin{aligned} |\Psi_j\rangle &= \int \int d\omega_s d\omega_i f_j(\omega_s, \omega_i) e^{i\theta_j(\omega_s)} \hat{a}_{s_j}^\dagger(\omega_s) \hat{a}_{i_j}^\dagger(\omega_i) |0\rangle \\ &= \sum_n \sqrt{\lambda_{j,n}} \int d\omega_s \phi_{j,n}(\omega_s) e^{i\theta_j(\omega_s)} \hat{a}_{s_j}^\dagger(\omega_s) \int d\omega_i \psi_{j,n}(\omega_i) \hat{a}_{i_j}^\dagger(\omega_i) |0\rangle \end{aligned} \quad (1)$$

where $j = 1(2)$ stands for the indices of the first (second) SPDC process and $\hat{a}_{s_j}^\dagger(\omega_s)$ and $\hat{a}_{i_j}^\dagger(\omega_i)$ are the creation operators for signal and idler photons with frequencies ω_s and ω_i . Here, we assume that the signal photon is heralded and passes through the dispersive medium of length L_j , so we have introduced the signal photon phase $\theta_j(\omega_s)$ to reflect the group velocity dispersion β_j as $\theta_j(\omega_s) = \frac{1}{2} L_j \beta_j \omega_s^2$. The terms $\phi_{j,n}(\omega_s)$ and the $\psi_{j,n}(\omega_i)$ are the Schmidt modes defined by

Schmidt decompositions of the joint spectral intensities, $f_j(\omega_s, \omega_i) = \sum_n \sqrt{\lambda_{j,n}} \phi_{j,n}(\omega_s) \psi_{j,n}(\omega_i)$ where $\lambda_{j,n}$ is the Schmidt eigenvalue. The heralding process will make the two-photon state into the reduced state in the density matrix form,

$$\rho_{sj} = \text{Tr}_i[|\Psi_j\rangle\langle\Psi_j|] = \sum_n \lambda_{j,n} |\phi_{j,n}\rangle\langle\phi_{j,n}| \quad (2)$$

where $|\phi_{j,n}\rangle = \int d\omega \phi_{j,n}(\omega) e^{-i\theta_j(\omega)} \hat{a}_{sj}^\dagger(\omega) |0\rangle$. Then, the two independent heralded single photon states before the beam splitter is described as

$$\rho^{in} = \rho_{s1} \otimes \rho_{s2} = \sum_{mm'} \lambda_{1,n} \lambda_{2,n'} (|\phi_{1,n}\rangle|\phi_{2,n'}\rangle)\langle\phi_{1,n}|\langle\phi_{2,n'}|. \quad (3)$$

After applying the relative optical time delay τ and the beam splitter unitary transformation of the creation operators, the output state ρ^{out} can be obtained. The coincidence probability P, between the two detectors D₃ and D₄ is given as

$$\begin{aligned} P &= \text{Tr}[\rho^{out} \hat{P}_{D_3} \otimes \hat{P}_{D_4}] \\ &= \frac{1}{2} - \frac{1}{2} \sum_{mm'} \lambda_{1,n} \lambda_{2,n'} \\ &\quad \times \int d\omega \phi_{1,n}(\omega) \phi_{2,n'}^*(\omega) e^{\frac{1}{2}i(\beta_1 L_1 - \beta_2 L_2)\omega^2} e^{i\omega\tau} \int d\omega' \phi_{1,n}^*(\omega') \phi_{2,n'}(\omega') e^{-\frac{1}{2}i(\beta_1 L_1 - \beta_2 L_2)\omega'^2} e^{-i\omega'\tau} \end{aligned} \quad (4)$$

where \hat{P}_{D_k} is the detection projector, $\hat{P}_{D_k} = \int d\omega \hat{b}_{sk}^\dagger(\omega) |0\rangle\langle 0| \hat{b}_{sk}(\omega)$ on the output mode of the beam splitter \hat{b}_{sk}^\dagger .

If one postulates a pure state of the heralded single photon without changing the spectrum, it can be obtained by summing up the all Schmidt modes after multiplying the Schmidt eigenvalues, $\tilde{\phi}_j = \sum_n \lambda_{j,n} \phi_{j,n}(\omega_s)$. By substituting the transformed Schmidt mode to the Eq. (2), the coincidence probability can be obtained with the pure state which has Schmidt number of unity satisfying $\lambda_{1,n} = \lambda_{2,n'} = 1$, but the spectrum of photon remains same. In general, however, the Schmidt decomposition cannot be done analytically. So, we numerically calculated joint spectral intensity which is the product of the pump spectral profile and the phase matching function of the nonlinear crystal and computed its singular value decomposition, which is the matrix analogue of the Schmidt decomposition. From the Eq. (4), one can easily find that the dispersion effect is perfectly cancelled out when $\beta_1 L_1 = \beta_2 L_2$ is satisfied. In addition, if one assumes that the two independent single-photons have the same spectral function $\phi_1 = \phi_2$, which corresponds to the case in our experiment, the coincidence probability can be simplified as

$$\begin{aligned} P(\tau \rightarrow 0) &= \frac{1}{2} - \frac{1}{2} \sum_{mm'} \lambda_{1,n} \lambda_{1,n'} \int d\omega \phi_{1,n}(\omega) \phi_{1,n'}^*(\omega) \int d\omega' \phi_{1,n}^*(\omega') \phi_{1,n'}(\omega') \\ &= \frac{1}{2} - \frac{1}{2} \sum_{mm'} \lambda_{1,n} \lambda_{1,n'} \int d\omega \phi_{1,n}(\omega) \phi_{1,n'}^*(\omega) \delta_{nn'} \\ &= \frac{1}{2} - \frac{1}{2} \sum_n \lambda_{1,n}^2, \end{aligned} \quad (5)$$

when the time delay τ goes to zero. As the purity of the heralded single-photon is given by $\text{Tr}[\rho_{sj}^2] = \sum_n \lambda_{j,n}^2$, the coincidence probability is only determined by the spectral purity of the single-photon when the dispersion is cancelled out.

In our experiment, especially, we used the identical optical fibers for dispersive media, thus dispersion cancellation only depends on the optical fiber length difference between two optical

fibers, $L_1 - L_2$. By following the Eq. (4), we calculate the coincidence probability as a function of τ as shown in Fig. 3 (dashed lines) and it is in good agreement with the experimental observations. In addition, to examine the effects of dispersion, we calculated the visibility and FWHM width of the two-photon interference dip as a function of the optical fiber length difference as shown in Fig. 4. Solid lines show the theoretical calculation following the experimental conditions where the heralded single photons are filtered by 10-nm FWHM bandwidth filters, so the single photon states are in the spectrally mixed state. As the optical fiber length difference is increased, the visibility is decreased and the FWHM bandwidth becomes broadened which results from the dispersion effect. If the heralded single photon states are in the spectrally pure state where the single photon has the same spectrum with the experimental condition, the dispersion is cancelled out and show the visibility of a unity when the optical fiber length difference is zero, but it shows the same tendency as the optical fiber length difference is increased (see the dashed lines in Fig. 4).

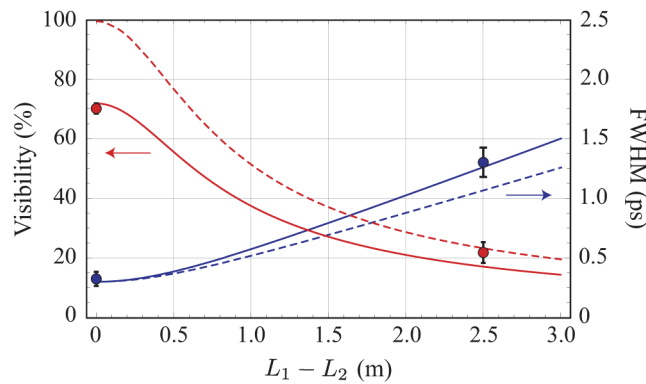


Fig. 4. Theoretical visibility and FWHM widths of the two-photon interference dip between two independent heralded single photons as a function of the optical fiber lengths difference. The solid lines show the theoretical results using the experimental condition when the heralded single photons are in spectrally mixed states. The dashed lines show the theoretical results for the heralded single photons in the spectrally pure states having the same bandwidths. The solid circles show the experimental data. The error bars represent one standard deviation, calculated from Poissonian counting statistics of the detection events.

3.2. Dispersion cancellation in a three-photon quantum interferometer

It is also interesting to consider the dispersion cancellation effect for the multi-path linear interferometer with N independent single photons. For instance, let us consider the scheme shown in Fig. 5 in which a single photon is injected into each input mode of a 3×3 linear interferometer which contains some dispersion elements. The single photon is assumed to be in a spectrally pure state described as,

$$|\phi\rangle_{a,b,c} = \int d\omega \phi_{a,b,c}(\omega) \hat{a}_{a,b,c}^\dagger(\omega) |0\rangle, \quad (6)$$

where $\phi_{a,b,c}(\omega)$ is the spectral function and $\hat{a}_{a,b,c}^\dagger(\omega)$ is the creation operator for photons of modes a , b , and c . Then, the total quantum state of the three single photons before arriving at the 50/50

beam splitter BS1 is described as

$$|\psi_{BS1}^{in}\rangle_{abc} = \int d\omega_1 \phi_a(\omega_1) \hat{a}_a^\dagger(\omega_1) e^{i\theta_1(\omega_1)} \int d\omega_2 \phi_b(\omega_2) \hat{a}_b^\dagger(\omega_2) e^{i\theta_2(\omega_2)} \times \int d\omega_3 \phi_c(\omega_3) \hat{a}_c^\dagger(\omega_3) e^{i\theta_3(\omega_3)} |0\rangle_{abc}, \quad (7)$$

for $\theta_i(\omega) = \frac{1}{2}L_i\beta_i\omega^2$ where β_i is the group velocity dispersion and L_i is the length of dispersive media. After passing through BS1, the creation operators transform accordingly, $\hat{a}_a^\dagger(\omega) \rightarrow \frac{1}{\sqrt{2}}(\hat{a}_a^\dagger(\omega) + \hat{a}_b^\dagger(\omega))$ and $\hat{a}_b^\dagger(\omega) \rightarrow \frac{1}{\sqrt{2}}(\hat{a}_a^\dagger(\omega) - \hat{a}_b^\dagger(\omega))$, thus the output state after BS1 becomes

$$|\psi_{BS1}^{out}\rangle_{abc} = \frac{1}{2} \int d\omega_1 \phi_a(\omega_1) e^{i\theta_1(\omega_1)} \int d\omega_2 \phi_b(\omega_2) e^{i\theta_2(\omega_2)} \int d\omega_3 \phi_c(\omega_3) e^{i\theta_3(\omega_3)} \times \left[\hat{a}_a^\dagger(\omega_1) \hat{a}_a^\dagger(\omega_2) + \hat{a}_a^\dagger(\omega_2) \hat{a}_b^\dagger(\omega_1) - \hat{a}_a^\dagger(\omega_1) \hat{a}_b^\dagger(\omega_2) - \hat{a}_b^\dagger(\omega_1) \hat{a}_b^\dagger(\omega_2) \right] \hat{a}_c^\dagger(\omega_3) |0\rangle_{abc}. \quad (8)$$

Another dispersive medium located between two BSs makes a transformation of the creation operator of mode a as $\hat{a}_a^\dagger(\omega) \rightarrow \hat{a}_a^\dagger(\omega) e^{i\theta_{12}(\omega)}$ and the total quantum state becomes

$$|\psi_{BS1}^{out}\rangle_{abc} = \frac{1}{2} \int d\omega_1 \phi_a(\omega_1) e^{i\theta_1(\omega_1)} \int d\omega_2 \phi_b(\omega_2) e^{i\theta_2(\omega_2)} \int d\omega_3 \phi_c(\omega_3) e^{i\theta_3(\omega_3)} \times \left[\hat{a}_a^\dagger(\omega_1) \hat{a}_a^\dagger(\omega_2) e^{i\theta_{12}(\omega_1)} e^{i\theta_{12}(\omega_2)} + \hat{a}_a^\dagger(\omega_2) \hat{a}_b^\dagger(\omega_1) e^{i\theta_{12}(\omega_2)} - \hat{a}_a^\dagger(\omega_1) \hat{a}_b^\dagger(\omega_2) e^{i\theta_{12}(\omega_1)} - \hat{a}_b^\dagger(\omega_1) \hat{a}_b^\dagger(\omega_2) \right] \hat{a}_c^\dagger(\omega_3) |0\rangle_{abc}. \quad (9)$$

After passing through BS2, the creation operators again transform accordingly, $\hat{a}_a^\dagger(\omega) \rightarrow \frac{1}{\sqrt{2}}(\hat{a}_a^\dagger(\omega) + \hat{a}_c^\dagger(\omega))$ and $\hat{a}_c^\dagger(\omega) \rightarrow \frac{1}{\sqrt{2}}(\hat{a}_a^\dagger(\omega) - \hat{a}_c^\dagger(\omega))$.

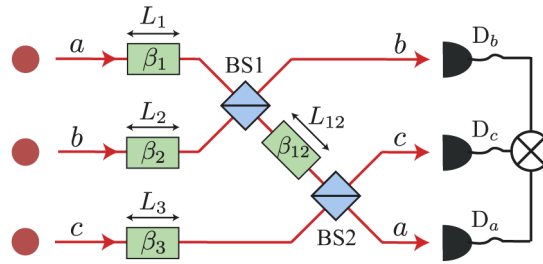


Fig. 5. Schematic of a multi-path quantum interferometer with three single photons and four dispersive media. Under specific sets of conditions, full dispersion cancellation for three-photon quantum interference can be achieved. Calculations show that the easiest way to achieve full dispersion cancellation for three-photon quantum interference is to satisfy the following conditions: $\beta_1 L_1 = \beta_2 L_2$ & $\beta_1 L_1 + \beta_{12} L_{12} = \beta_3 L_3$.

Finally, the output state of the 3×3 quantum interferometer is given as,

$$\begin{aligned}
 |\psi_{\text{BS2}}^{\text{out}}\rangle_{abc} = & \frac{1}{2} \int d\omega_1 \int d\omega_2 \int d\omega_3 \phi_a(\omega_1) \phi_b(\omega_2) \phi_c(\omega_3) e^{i(\theta_1(\omega_1) + \theta_2(\omega_2) + \theta_3(\omega_3))} \\
 & \times \left[\frac{1}{2} (\hat{a}_a^\dagger(\omega_1) + \hat{a}_c^\dagger(\omega_1)) (\hat{a}_a^\dagger(\omega_2) + \hat{a}_c^\dagger(\omega_2)) e^{i(\theta_{12}(\omega_1) + \theta_{12}(\omega_2))} \right. \\
 & + \frac{1}{\sqrt{2}} (\hat{a}_a^\dagger(\omega_2) + \hat{a}_c^\dagger(\omega_2)) \hat{a}_b^\dagger(\omega_1) e^{i\theta_{12}(\omega_2)} - \frac{1}{\sqrt{2}} (\hat{a}_a^\dagger(\omega_1) + \hat{a}_c^\dagger(\omega_1)) \hat{a}_b^\dagger(\omega_2) e^{i\theta_{12}(\omega_1)} \\
 & \left. - \hat{a}_b^\dagger(\omega_1) \hat{a}_b^\dagger(\omega_2) \right] \times \frac{1}{\sqrt{2}} (\hat{a}_a^\dagger(\omega_3) - \hat{a}_c^\dagger(\omega_3)) |0\rangle_{abc}.
 \end{aligned} \tag{10}$$

The coincidence probability P , among the three detectors D_a , D_b , and D_c is given as

$$P = {}_{abc} \langle \psi_{\text{BS2}}^{\text{out}} | \hat{P}_a \otimes \hat{P}_b \otimes \hat{P}_c | \psi_{\text{BS2}}^{\text{out}} \rangle_{abc}, \tag{11}$$

where \hat{P}_i is the projector defined as $\hat{P}_i = \int d\omega \hat{a}_i^\dagger(\omega) |0\rangle_{ii} \langle 0| \hat{a}_i(\omega)$ on the output mode $i = a, b, c$. Calculating Eq. (11) by substituting Eq. (10) leads to the coincidence probability,

$$\begin{aligned}
 P = & \frac{1}{16} \left[4 - 4 \left| \int d\omega \phi_a(\omega) \phi_b^*(\omega) e^{i(\theta_1(\omega) - \theta_2(\omega))} \right|^2 - 2 \left| \int d\omega \phi_b(\omega) \phi_c^*(\omega) e^{i(\theta_2(\omega) - \theta_3(\omega) + \theta_{12}(\omega))} \right|^2 \right. \\
 & - 2 \left| \int d\omega \phi_c(\omega) \phi_a^*(\omega) e^{i(\theta_3(\omega) - \theta_1(\omega) - \theta_{12}(\omega))} \right|^2 + 2 \int d\omega \phi_a(\omega) \phi_b^*(\omega) e^{i(\theta_1(\omega) - \theta_2(\omega))} \\
 & \times \int d\omega \phi_b(\omega) \phi_c^*(\omega) e^{i(\theta_2(\omega) - \theta_3(\omega) + \theta_{12}(\omega))} \int d\omega \phi_c(\omega) \phi_a^*(\omega) e^{i(\theta_3(\omega) - \theta_1(\omega) - \theta_{12}(\omega))} \\
 & + 2 \int d\omega \phi_a^*(\omega) \phi_b(\omega) e^{-i(\theta_1(\omega) - \theta_2(\omega))} \int d\omega \phi_b^*(\omega) \phi_c(\omega) e^{-i(\theta_2(\omega) - \theta_3(\omega) + \theta_{12}(\omega))} \\
 & \left. \times \int d\omega \phi_c^*(\omega) \phi_a(\omega) e^{-i(\theta_3(\omega) - \theta_1(\omega) - \theta_{12}(\omega))} \right].
 \end{aligned} \tag{12}$$

If the single photons initially have the identical spectra, the coincidence probability P is calculated to be

$$\begin{aligned}
 P = & \frac{1}{16} \left[4 - 4 \left| \int d\omega |\phi(\omega)|^2 e^{i(\theta_1(\omega) - \theta_2(\omega))} \right|^2 - 2 \left| \int d\omega |\phi(\omega)|^2 e^{i(\theta_2(\omega) - \theta_3(\omega) + \theta_{12}(\omega))} \right|^2 \right. \\
 & - 2 \left| \int d\omega |\phi(\omega)|^2 e^{i(\theta_3(\omega) - \theta_1(\omega) - \theta_{12}(\omega))} \right|^2 + 2 \int d\omega |\phi(\omega)|^2 e^{i(\theta_1(\omega) - \theta_2(\omega))} \\
 & \times \int d\omega |\phi(\omega)|^2 e^{i(\theta_2(\omega) - \theta_3(\omega) + \theta_{12}(\omega))} \int d\omega |\phi(\omega)|^2 e^{i(\theta_3(\omega) - \theta_1(\omega) - \theta_{12}(\omega))} \\
 & + 2 \int d\omega |\phi(\omega)|^2 e^{-i(\theta_1(\omega) - \theta_2(\omega))} \int d\omega |\phi(\omega)|^2 e^{-i(\theta_2(\omega) - \theta_3(\omega) + \theta_{12}(\omega))} \\
 & \left. \times \int d\omega |\phi(\omega)|^2 e^{-i(\theta_3(\omega) - \theta_1(\omega) - \theta_{12}(\omega))} \right].
 \end{aligned} \tag{13}$$

Since the optical delays are assumed to be matched, if the dispersion effects are fully cancelled out, the coincidence probability P should become zero. To figure out the conditions for dispersion

cancellation, we first assume $\theta_1(\omega) = \theta_2(\omega)$ at which case the coincidence probability is given by

$$\begin{aligned}
 P = \frac{1}{8} & \left[- \left| \int d\omega |\phi(\omega)|^2 e^{i(\theta_1(\omega) - \theta_3(\omega) + \theta_{12}(\omega))} \right|^2 - \left| \int d\omega |\phi(\omega)|^2 e^{i(\theta_3(\omega) - \theta_1(\omega) - \theta_{12}(\omega))} \right|^2 \right. \\
 & + \int d\omega |\phi(\omega)|^2 e^{i(\theta_1(\omega) - \theta_3(\omega) + \theta_{12}(\omega))} \int d\omega |\phi(\omega)|^2 e^{i(\theta_3(\omega) - \theta_1(\omega) - \theta_{12}(\omega))} \\
 & \left. + \int d\omega |\phi(\omega)|^2 e^{-i(\theta_1(\omega) - \theta_3(\omega) + \theta_{12}(\omega))} \int d\omega |\phi(\omega)|^2 e^{-i(\theta_3(\omega) - \theta_1(\omega) - \theta_{12}(\omega))} \right]. \quad (14)
 \end{aligned}$$

From the above equation, it is found that P goes to zero for the condition $\theta_1(\omega) + \theta_{12}(\omega) = \theta_3(\omega)$. Therefore, we find that there is a condition for dispersion cancellation for a three-photon quantum interferometer: $\beta_1 L_1 = \beta_2 L_2$ & $\beta_1 L_1 + \beta_{12} L_{12} = \beta_3 L_3$. The condition for dispersion cancellation in the case of the four-photon quantum interferometer is also shown in [Appendix](#). Similarly, the condition for dispersion cancellation in the case of the N -photon quantum interferometer can be found.

3.3. Dispersion cancellation in an N -photon quantum interferometer

In this section, we consider the case where there are N independent but identically-prepared single photons at the input of a specific form of the $N \times N$ interferometer within which there are dispersive elements as shown in [Fig. 6](#).

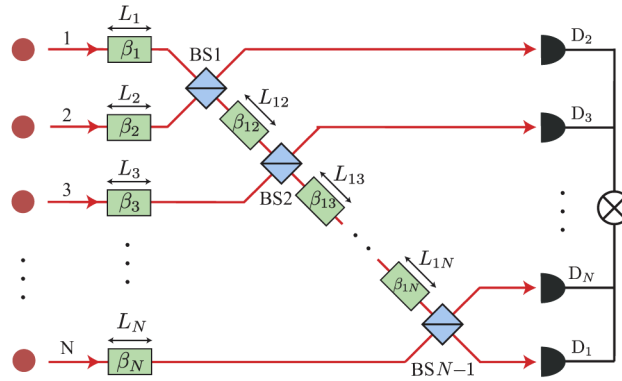


Fig. 6. Schematic of the simplest multi-path quantum interferometer with N single photons. Under specific sets of condition, full dispersion cancellation for N -photon quantum interference can be achieved.

The total quantum state before arriving at the BS1 is described as

$$|\phi_{\text{BS1}}^{\text{in}}\rangle = \int \prod_{j=1}^N d\omega_j \phi(\omega_j) \hat{a}_j^\dagger(\omega_j) e^{i\theta_j(\omega_j)} |0\rangle. \quad (15)$$

Each time the photons pass through BSs, the creation operators transform accordingly, $\hat{a}_1^\dagger(\omega) \rightarrow \frac{1}{\sqrt{2}}(e^{i\theta_{1j}(\omega)} \hat{a}_1^\dagger(\omega) + \hat{a}_j^\dagger(\omega))$ and $\hat{a}_j^\dagger(\omega) \rightarrow \frac{1}{\sqrt{2}}(e^{i\theta_{1j}(\omega)} \hat{a}_1^\dagger(\omega) - \hat{a}_j^\dagger(\omega))$ for $j = 2, \dots, N-1$, and after passing through the last BS, the creation operators transform accordingly, $\hat{a}_1^\dagger(\omega) \rightarrow \frac{1}{\sqrt{2}}(\hat{a}_1^\dagger(\omega) + \hat{a}_N^\dagger(\omega))$ and $\hat{a}_N^\dagger(\omega) \rightarrow \frac{1}{\sqrt{2}}(\hat{a}_1^\dagger(\omega) - \hat{a}_N^\dagger(\omega))$.

Then, the output state of the $N \times N$ quantum interferometer and the coincidence probability can be obtained by following the calculation strategy shown in Subsection 3.2 and [Appendix](#). Finally, it can be found that the dispersion cancellation effect where the coincidence probability becomes zero can be achieved for N -photon quantum interferometer: $\beta_1 L_1 = \beta_2 L_2$ & $\beta_1 L_1 + \beta_{12} L_{12} = \beta_3 L_3$ & \dots & $\beta_1 L_1 + \sum_{j=2}^N \beta_{1j} L_{1j} = \beta_N L_N$.

4. Conclusion

In conclusion, we have experimentally and theoretically investigated the dispersion effect on quantum interference between two independent single photons and showed that it is possible to achieve full dispersion cancellation even with the independent single photons experiencing heavy group velocity dispersion as long as the photons experience the same amount of dispersion. We have also shown that the dispersion cancellation in quantum interference can be applied to N -photon quantum circuits and networks. Since multi-port quantum interferometers are at the heart of photonic quantum devices for quantum communication, quantum computing, and quantum simulation, we believe that our work would have wide applicability in quantum information science.

Note added: A similar dispersion cancellation effect has recently been reported for two laser wave packets [45].

Appendix

Consider the dispersion cancellation in a four-photon quantum interferometer as shown in Fig. 7 which contains some dispersion elements. The total quantum state of the four single photons before arriving at the BS1 is described as

$$|\phi_{\text{BS1}}^{\text{in}}\rangle_{abcd} = \int d\omega_1 \phi_a(\omega_1) \hat{a}_a^\dagger(\omega_1) e^{i\theta_1(\omega_1)} \int d\omega_2 \phi_b(\omega_2) \hat{a}_b^\dagger(\omega_2) e^{i\theta_2(\omega_2)} \\ \times \int d\omega_3 \phi_c(\omega_3) \hat{a}_c^\dagger(\omega_3) e^{i\theta_3(\omega_3)} \int d\omega_4 \phi_d(\omega_4) \hat{a}_d^\dagger(\omega_4) e^{i\theta_4(\omega_4)} |0\rangle_{abcd} \quad (16)$$

After passing through the series of BSs, the creation operators transform successively, (i) $\hat{a}_a^\dagger(\omega) \rightarrow \frac{1}{\sqrt{2}}(e^{i\theta_{12}(\omega)} \hat{a}_a^\dagger(\omega) + \hat{a}_b^\dagger(\omega))$ and $\hat{a}_b^\dagger(\omega) \rightarrow \frac{1}{\sqrt{2}}(e^{i\theta_{12}(\omega)} \hat{a}_a^\dagger(\omega) - \hat{a}_b^\dagger(\omega))$, (ii) $\hat{a}_a^\dagger(\omega) \rightarrow \frac{1}{\sqrt{2}}(e^{i\theta_{13}(\omega)} \hat{a}_a^\dagger(\omega) + \hat{a}_c^\dagger(\omega))$ and $\hat{a}_c^\dagger(\omega) \rightarrow \frac{1}{\sqrt{2}}(e^{i\theta_{13}(\omega)} \hat{a}_a^\dagger(\omega) - \hat{a}_c^\dagger(\omega))$, (iii) $\hat{a}_a^\dagger(\omega) \rightarrow \frac{1}{\sqrt{2}}(\hat{a}_a^\dagger(\omega) + \hat{a}_d^\dagger(\omega))$ and $\hat{a}_d^\dagger(\omega) \rightarrow \frac{1}{\sqrt{2}}(\hat{a}_a^\dagger(\omega) - \hat{a}_d^\dagger(\omega))$.

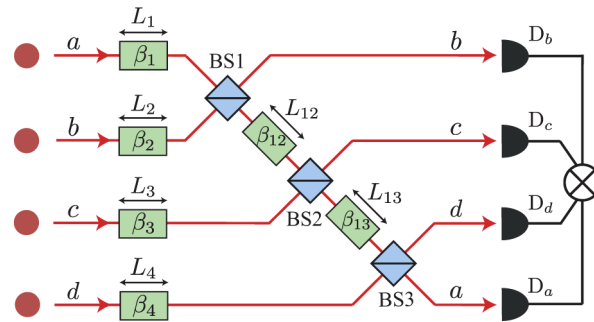


Fig. 7. Schematic of a multi-path quantum interferometer with four single photons and six dispersive media. Under specific sets of conditions, full dispersion cancellation for four-photon quantum interference can be achieved. Calculations show that the easiest way to achieve full dispersion cancellation for four-photon quantum interference is to satisfy the following conditions: $\beta_1 L_1 = \beta_2 L_2$ & $\beta_1 L_1 + \beta_{12} L_{12} = \beta_3 L_3$ & $\beta_1 L_1 + \beta_{12} L_{12} + \beta_{13} L_{13} = \beta_4 L_4$.

Finally, the output state of the 4×4 quantum interferometer is given as,

$$\begin{aligned}
|\phi_{\text{BS3}}^{\text{out}}\rangle_{abcd} &= \frac{1}{4} \int d\omega_1 d\omega_2 d\omega_3 d\omega_4 \phi_a(\omega_1) \phi_b(\omega_2) \phi_c(\omega_3) \phi_d(\omega_4) e^{i(\theta_1(\omega_1) + \theta_2(\omega_2) + \theta_3(\omega_3) + \theta_4(\omega_4))} \\
&\times \left[\frac{1}{2\sqrt{2}} \left(\frac{1}{2\sqrt{2}} (\hat{a}_a^\dagger(\omega_1) + \hat{a}_d^\dagger(\omega_1)) (\hat{a}_a^\dagger(\omega_2) + \hat{a}_d^\dagger(\omega_2)) (\hat{a}_a^\dagger(\omega_3) + \hat{a}_d^\dagger(\omega_3)) e^{i(\theta_{13}(\omega_1) + \theta_{13}(\omega_2) + \theta_{13}(\omega_3))} \right. \right. \\
&+ \frac{1}{2} (\hat{a}_a^\dagger(\omega_1) + \hat{a}_d^\dagger(\omega_1)) (\hat{a}_a^\dagger(\omega_3) + \hat{a}_d^\dagger(\omega_3)) \hat{a}_c^\dagger(\omega_2) e^{i(\theta_{13}(\omega_1) + \theta_{13}(\omega_3))} \\
&+ \frac{1}{2} (\hat{a}_a^\dagger(\omega_2) + \hat{a}_d^\dagger(\omega_2)) (\hat{a}_a^\dagger(\omega_3) + \hat{a}_d^\dagger(\omega_3)) \hat{a}_c^\dagger(\omega_1) e^{i(\theta_{13}(\omega_2) + \theta_{13}(\omega_3))} \\
&+ \frac{1}{\sqrt{2}} (\hat{a}_a^\dagger(\omega_3) + \hat{a}_d^\dagger(\omega_3)) \hat{a}_c^\dagger(\omega_1) \hat{a}_c^\dagger(\omega_2) e^{i\theta_{13}(\omega_3)} \left. \right) \times e^{i(\theta_{12}(\omega_1) + \theta_{12}(\omega_2))} \\
&+ \frac{1}{2} \left(\frac{1}{2} (\hat{a}_a^\dagger(\omega_2) + \hat{a}_d^\dagger(\omega_2)) (\hat{a}_a^\dagger(\omega_3) + \hat{a}_d^\dagger(\omega_3)) \hat{a}_b^\dagger(\omega_1) e^{i(\theta_{13}(\omega_2) + \theta_{13}(\omega_3))} \right. \\
&+ \frac{1}{\sqrt{2}} (\hat{a}_a^\dagger(\omega_3) + \hat{a}_d^\dagger(\omega_3)) \hat{a}_b^\dagger(\omega_1) \hat{a}_c^\dagger(\omega_2) e^{i\theta_{13}(\omega_3)} \left. \right) \times e^{i\theta_{12}(\omega_2)} \\
&- \frac{1}{2} \left(\frac{1}{2} (\hat{a}_a^\dagger(\omega_1) + \hat{a}_d^\dagger(\omega_1)) (\hat{a}_a^\dagger(\omega_3) + \hat{a}_d^\dagger(\omega_3)) \hat{a}_b^\dagger(\omega_2) e^{i(\theta_{13}(\omega_1) + \theta_{13}(\omega_3))} \right. \\
&+ \frac{1}{\sqrt{2}} (\hat{a}_a^\dagger(\omega_3) + \hat{a}_d^\dagger(\omega_3)) \hat{a}_b^\dagger(\omega_2) \hat{a}_c^\dagger(\omega_1) e^{i\theta_{13}(\omega_3)} \left. \right) \times e^{i\theta_{12}(\omega_1)} \\
&- \frac{1}{2} (\hat{a}_a^\dagger(\omega_3) + \hat{a}_d^\dagger(\omega_3)) \hat{a}_b^\dagger(\omega_1) \hat{a}_b^\dagger(\omega_2) \times e^{i\theta_{13}(\omega_3)} \\
&- \frac{1}{2\sqrt{2}} \left(\frac{1}{2} (\hat{a}_a^\dagger(\omega_1) + \hat{a}_d^\dagger(\omega_1)) (\hat{a}_a^\dagger(\omega_2) + \hat{a}_d^\dagger(\omega_2)) \hat{a}_c^\dagger(\omega_3) e^{i(\theta_{13}(\omega_1) + \theta_{13}(\omega_2))} \right. \\
&+ \frac{1}{\sqrt{2}} (\hat{a}_a^\dagger(\omega_1) + \hat{a}_d^\dagger(\omega_1)) \hat{a}_c^\dagger(\omega_2) \hat{a}_c^\dagger(\omega_3) e^{i\theta_{13}(\omega_1)} \\
&+ \frac{1}{\sqrt{2}} (\hat{a}_a^\dagger(\omega_2) + \hat{a}_d^\dagger(\omega_2)) \hat{a}_c^\dagger(\omega_1) \hat{a}_c^\dagger(\omega_3) e^{i\theta_{13}(\omega_2)} \\
&+ \hat{a}_c^\dagger(\omega_1) \hat{a}_c^\dagger(\omega_2) \hat{a}_c^\dagger(\omega_3) \left. \right) \times e^{i(\theta_{12}(\omega_1) + \theta_{12}(\omega_2))} \\
&- \frac{1}{2} \left(\frac{1}{\sqrt{2}} (\hat{a}_a^\dagger(\omega_2) + \hat{a}_d^\dagger(\omega_2)) \hat{a}_b^\dagger(\omega_1) \hat{a}_c^\dagger(\omega_3) e^{i\theta_{13}(\omega_2)} + \hat{a}_b^\dagger(\omega_1) \hat{a}_c^\dagger(\omega_2) \hat{a}_c^\dagger(\omega_3) \right) \times e^{i\theta_{12}(\omega_2)} \\
&+ \frac{1}{2} \left(\frac{1}{\sqrt{2}} (\hat{a}_a^\dagger(\omega_1) + \hat{a}_d^\dagger(\omega_1)) \hat{a}_b^\dagger(\omega_2) \hat{a}_c^\dagger(\omega_3) e^{i\theta_{13}(\omega_1)} + \hat{a}_b^\dagger(\omega_2) \hat{a}_c^\dagger(\omega_1) \hat{a}_c^\dagger(\omega_3) \right) \times e^{i\theta_{12}(\omega_1)} \\
&+ \frac{1}{\sqrt{2}} \hat{a}_b^\dagger(\omega_1) \hat{a}_b^\dagger(\omega_2) \hat{a}_c^\dagger(\omega_3) \left. \right] (\hat{a}_a^\dagger(\omega_4) - \hat{a}_d^\dagger(\omega_4)) |0\rangle_{abcd}
\end{aligned} \tag{17}$$

The coincidence probability P , among the four detectors D_a , D_b , D_c , and D_d is given as

$$P = {}_{abcd} \langle \psi_{\text{BS2}}^{\text{out}} | \hat{P}_a \otimes \hat{P}_b \otimes \hat{P}_c \otimes \hat{P}_d | \psi_{\text{BS2}}^{\text{out}} \rangle_{abcd}. \tag{18}$$

Calculating Eq. (18) by substituting Eq. (17) leads to the coincidence probability,

$$\begin{aligned}
P = & \frac{1}{128} \left[8 - 4 \left| \int d\omega |\phi(\omega)|^2 e^{-i\theta_{13}(\omega)} e^{-i\theta_3(\omega)} e^{i\theta_4(\omega)} \right|^2 - 8 \left| \int d\omega |\phi(\omega)|^2 e^{-i\theta_1(\omega)} e^{i\theta_2(\omega)} \right|^2 \right. \\
& + 4 \left| \int d\omega |\phi(\omega)|^2 e^{-i\theta_2(\omega)} e^{i\theta_1(\omega)} \right|^2 \times \left| \int d\omega |\phi(\omega)|^2 e^{-i\theta_4(\omega)} e^{i\theta_3(\omega)} e^{i\theta_{13}(\omega)} \right|^2 \\
& - 4 \left| \int d\omega |\phi(\omega)|^2 e^{-i\theta_3(\omega)} e^{i\theta_2(\omega)} e^{i\theta_{12}(\omega)} \right|^2 \\
& + 2 \int d\omega |\phi(\omega)|^2 e^{-i\theta_3(\omega)} e^{i\theta_2(\omega)} e^{i\theta_{12}(\omega)} \times \int d\omega |\phi(\omega)|^2 e^{-i\theta_4(\omega)} e^{i\theta_3(\omega)} e^{i\theta_{13}(\omega)} \\
& \times \int d\omega |\phi(\omega)|^2 e^{-i\theta_2(\omega)} e^{i\theta_4(\omega)} e^{-i\theta_{13}(\omega)} e^{-i\theta_{12}(\omega)} \\
& + 4 \int d\omega |\phi(\omega)|^2 e^{-i\theta_2(\omega)} e^{i\theta_1(\omega)} \times \int d\omega |\phi(\omega)|^2 e^{-i\theta_3(\omega)} e^{i\theta_2(\omega)} e^{i\theta_{12}(\omega)} \\
& \times \int d\omega |\phi(\omega)|^2 e^{-i\theta_1(\omega)} e^{i\theta_3(\omega)} e^{-i\theta_{12}(\omega)} \\
& - 2 \int d\omega |\phi(\omega)|^2 e^{-i\theta_2(\omega)} e^{i\theta_1(\omega)} \times \int d\omega |\phi(\omega)|^2 e^{-i\theta_1(\omega)} e^{i\theta_4(\omega)} e^{-i\theta_{13}(\omega)} e^{-i\theta_{12}(\omega)} \\
& \times \int d\omega |\phi(\omega)|^2 e^{-i\theta_4(\omega)} e^{i\theta_3(\omega)} e^{i\theta_{13}(\omega)} \times \int d\omega |\phi(\omega)|^2 e^{-i\theta_3(\omega)} e^{i\theta_2(\omega)} e^{i\theta_{12}(\omega)} \\
& 2 \int d\omega |\phi(\omega)|^2 e^{-i\theta_4(\omega)} e^{i\theta_1(\omega)} e^{i\theta_{13}(\omega)} e^{i\theta_{12}(\omega)} \times \int d\omega |\phi(\omega)|^2 e^{-i\theta_1(\omega)} e^{i\theta_2(\omega)} \\
& \times \int d\omega |\phi(\omega)|^2 e^{-i\theta_2(\omega)} e^{i\theta_3(\omega)} e^{-i\theta_{12}(\omega)} \times \int d\omega |\phi(\omega)|^2 e^{-i\theta_3(\omega)} e^{i\theta_4(\omega)} e^{-i\theta_{13}(\omega)} \\
& + 4 \int d\omega |\phi(\omega)|^2 e^{-i\theta_3(\omega)} e^{i\theta_1(\omega)} e^{i\theta_{12}(\omega)} \times \int d\omega |\phi(\omega)|^2 e^{-i\theta_1(\omega)} e^{i\theta_2(\omega)} \\
& \times \int d\omega |\phi(\omega)|^2 e^{-i\theta_2(\omega)} e^{i\theta_3(\omega)} e^{-i\theta_{12}(\omega)} \\
& + 2 \int d\omega |\phi(\omega)|^2 e^{-i\theta_4(\omega)} e^{i\theta_1(\omega)} e^{i\theta_{13}(\omega)} e^{i\theta_{12}(\omega)} \times \int d\omega |\phi(\omega)|^2 e^{-i\theta_1(\omega)} e^{i\theta_3(\omega)} e^{-i\theta_{12}(\omega)} \\
& \times \int d\omega |\phi(\omega)|^2 e^{-i\theta_3(\omega)} e^{i\theta_4(\omega)} e^{-i\theta_{13}(\omega)} \\
& - 4 \left| \int d\omega |\phi(\omega)|^2 e^{-i\theta_3(\omega)} e^{i\theta_1(\omega)} e^{i\theta_{12}(\omega)} \right|^2 \\
& + 2 \int d\omega |\phi(\omega)|^2 e^{-i\theta_4(\omega)} e^{i\theta_1(\omega)} e^{i\theta_{13}(\omega)} e^{i\theta_{12}(\omega)} \times \int d\omega |\phi(\omega)|^2 e^{-i\theta_1(\omega)} e^{i\theta_2(\omega)} \\
& \times \int d\omega |\phi(\omega)|^2 e^{-i\theta_2(\omega)} e^{i\theta_4(\omega)} e^{-i\theta_{13}(\omega)} e^{-i\theta_{12}(\omega)} \\
& - 2 \left| \int d\omega |\phi(\omega)|^2 e^{-i\theta_4(\omega)} e^{i\theta_1(\omega)} e^{i\theta_{13}(\omega)} e^{i\theta_{12}(\omega)} \right|^2 \\
& + 2 \int d\omega |\phi(\omega)|^2 e^{-i\theta_4(\omega)} e^{i\theta_2(\omega)} e^{i\theta_{13}(\omega)} e^{i\theta_{12}(\omega)} \times \int d\omega |\phi(\omega)|^2 e^{-i\theta_2(\omega)} e^{i\theta_4(\omega)} e^{-i\theta_{12}(\omega)} \\
& \times \int d\omega |\phi(\omega)|^2 e^{-i\theta_3(\omega)} e^{i\theta_4(\omega)} e^{-i\theta_{13}(\omega)}
\end{aligned}$$

$$\begin{aligned}
& - 2 \int d\omega |\phi(\omega)|^2 e^{-i\theta_2(\omega)} e^{i\theta_1(\omega)} \times \int d\omega |\phi(\omega)|^2 e^{-i\theta_4(\omega)} e^{i\theta_2(\omega)} e^{i\theta_{13}(\omega)} e^{i\theta_{12}(\omega)} \\
& \times \int d\omega |\phi(\omega)|^2 e^{-i\theta_1(\omega)} e^{i\theta_3(\omega)} e^{-i\theta_{12}(\omega)} \times \int d\omega |\phi(\omega)|^2 e^{-i\theta_3(\omega)} e^{i\theta_4(\omega)} e^{-i\theta_{13}(\omega)} \\
& - 2 \left| \int d\omega |\phi(\omega)|^2 e^{-i\theta_4(\omega)} e^{i\theta_2(\omega)} e^{i\theta_{12}(\omega)} e^{i\theta_{13}(\omega)} \right|^2 \\
& + 2 \int d\omega |\phi(\omega)|^2 e^{-i\theta_2(\omega)} e^{i\theta_1(\omega)} \times \int d\omega |\phi(\omega)|^2 e^{-i\theta_4(\omega)} e^{i\theta_2(\omega)} e^{i\theta_{12}(\omega)} e^{i\theta_{13}(\omega)} \\
& \times \int d\omega |\phi(\omega)|^2 e^{-i\theta_1(\omega)} e^{i\theta_4(\omega)} e^{-i\theta_{12}(\omega)} e^{-i\theta_{13}(\omega)} \\
& - 2 \int d\omega |\phi(\omega)|^2 e^{-i\theta_3(\omega)} e^{i\theta_1(\omega)} e^{i\theta_{12}(\omega)} \times \int d\omega |\phi(\omega)|^2 e^{-i\theta_1(\omega)} e^{i\theta_2(\omega)} \\
& \times \int d\omega |\phi(\omega)|^2 e^{-i\theta_4(\omega)} e^{i\theta_3(\omega)} e^{i\theta_{13}(\omega)} \times \int d\omega |\phi(\omega)|^2 e^{-i\theta_2(\omega)} e^{i\theta_4(\omega)} e^{-i\theta_{13}(\omega)} e^{-i\theta_{12}(\omega)} \\
& + 2 \int d\omega |\phi(\omega)|^2 e^{-i\theta_3(\omega)} e^{i\theta_1(\omega)} e^{i\theta_{12}(\omega)} \times \int d\omega |\phi(\omega)|^2 e^{-i\theta_4(\omega)} e^{i\theta_3(\omega)} e^{i\theta_{13}(\omega)} \\
& \times \int d\omega |\phi(\omega)|^2 e^{-i\theta_1(\omega)} e^{i\theta_4(\omega)} e^{-i\theta_{13}(\omega)} e^{-i\theta_{12}(\omega)} \Big]
\end{aligned} \tag{19}$$

under the condition that the single photons have the same spectrum.

Since the optical delays are assumed to be matched, if the dispersion effects are fully cancelled out, the coincidence probability P should become zero. It is found that P goes to zero for the conditions $\theta_1(\omega) = \theta_2(\omega)$ and $\theta_1(\omega) + \theta_{12}(\omega) = \theta_3(\omega)$ and $\theta_1(\omega) + \theta_{12}(\omega) + \theta_{13}(\omega) = \theta_4(\omega)$. Therefore, we find that there is a condition for dispersion cancellation for the four-photon quantum interferometer: $\beta_1 L_1 = \beta_2 L_2$ & $\beta_1 L_1 + \beta_{12} L_{12} = \beta_3 L_3$ & $\beta_1 L_1 + \beta_{12} L_{12} + \beta_{13} L_{13} = \beta_4 L_4$.

Funding. Ministry of Science and ICT, South Korea (IITP-2020-0-01606); Agency for Defense Development (UG190028RD); National Research Foundation of Korea (2019R1A2C3004812).

Disclosures. The authors declare that there are no conflicts of interest related to this article.

References

1. N. Gisin and R. Thew, "Quantum communication," *Nat. Photonics* **1**(3), 165–171 (2007).
2. R. Ursin, F. Tiefenbacher, T. Schmitt-Manderbach, H. Weier, T. Scheidl, M. Lindenthal, B. Blauensteiner, T. Jennewein, J. Perdigues, P. Trojek, B. Ömer, M. Fürst, M. Meyenburg, J. Rarity, Z. Sodnik, C. Barbieri, H. Weinfurter, and A. Zeilinger, "Entanglement-based quantum communication over 144 km," *Nat. Phys.* **3**(7), 481–486 (2007).
3. C. H. Bennett, G. Brassard, C. Crépeau, R. Jozsa, A. Peres, and W. K. Wootters, "Teleporting an unknown quantum state via dual classical and Einstein-Podolsky-Rosen channels," *Phys. Rev. Lett.* **70**(13), 1895–1899 (1993).
4. D. Bouwmeester, J.-W. Pan, K. Mattle, M. Eibl, H. Weinfurter, and A. Zeilinger, "Experimental quantum teleportation," *Nature* **390**(6660), 575–579 (1997).
5. Y.-H. Kim, S. P. Kulik, and Y. Shih, "Quantum teleportation of a polarization state with a complete Bell state measurement," *Phys. Rev. Lett.* **86**(7), 1370–1373 (2001).
6. X.-L. Wang, X.-D. Cai, Z.-E. Su, M.-C. Chen, D. Wu, L. Li, N.-L. Liu, C.-Y. Lu, and J.-W. Pan, "Quantum teleportation of multiple degrees of freedom of a single photon," *Nature* **518**(7540), 516–519 (2015).
7. T. B. Pittman, Y. H. Shih, D. V. Strekalov, and A. V. Sergienko, "Optical imaging by means of two-photon quantum entanglement," *Phys. Rev. A* **52**(5), R3429–R3432 (1995).
8. D. V. Strekalov, A. V. Sergienko, D. N. Klyshko, and Y. H. Shih, "Observation of two-photon "Ghost" interference and diffraction," *Phys. Rev. Lett.* **74**(18), 3600–3603 (1995).
9. M. D'Angelo, Y.-H. Kim, S. P. Kulik, and Y. Shih, "Identifying entanglement using quantum ghost interference and imaging," *Phys. Rev. Lett.* **92**(23), 233601 (2004).
10. G. Brida, M. Genovese, and I. R. Berchera, "Experimental realization of sub-shot-noise quantum imaging," *Nat. Photonics* **4**(4), 227–230 (2010).
11. V. Giovannetti, S. Lloyd, and L. Maccone, "Advances in quantum metrology," *Nat. Photonics* **5**(4), 222–229 (2011).
12. P. Kok, W. J. Munro, K. Nemoto, T. C. Ralph, J. P. Dowling, and G. J. Milburn, "Linear optical quantum computing with photonic qubits," *Rev. Mod. Phys.* **79**(1), 135–174 (2007).

13. X.-C. Yao, T.-X. Wang, H.-Z. Chen, W.-B. Gao, A. G. Fowler, R. Raussendorf, Z.-B. Chen, N.-L. Liu, C.-Y. Lu, Y.-J. Deng, Y.-A. Chen, and J.-W. Pan, "Experimental demonstration of topological error correction," *Nature* **482**(7386), 489–494 (2012).
14. A. Valencia, M. V. Chekhova, A. Trifonov, and Y. Shih, "Entangled two-photon wave packet in a dispersive medium," *Phys. Rev. Lett.* **88**(18), 183601 (2002).
15. G. Brida, M. V. Chekhova, M. Genovese, M. Gramegna, and L. A. Krivitsky, "Dispersion spreading of biphotons in optical fibers and two-photon interference," *Phys. Rev. Lett.* **96**(14), 143601 (2006).
16. S.-Y. Baek, O. Kwon, and Y.-H. Kim, "Nonlocal dispersion control of a single-photon waveform," *Phys. Rev. A* **78**(1), 013816 (2008).
17. G. Brida, M. V. Chekhova, I. P. Degiovanni, M. Genovese, G. Kh. Kitaeva, A. Meda, and O. A. Shumilkina, "Chirped biphotons and their compression in optical fibers," *Phys. Rev. Lett.* **103**(19), 193602 (2009).
18. X. Ma, X. Li, L. Cui, X. Guo, and L. Yang, "Effect of chromatic-dispersion-induced chirp on the temporal coherence properties of individual beams from spontaneous four-wave mixing," *Phys. Rev. A* **84**(2), 023829 (2011).
19. X. Ma, L. Cui, and X. Li, "Hong-Ou-Mandel interference between independent sources of heralded ultrafast single photons: influence of chirp," *J. Opt. Soc. Am. B* **32**(5), 946 (2015).
20. K.-H. Hong, S.-Y. Baek, O. Kwon, and Y.-H. Kim, "Dispersive broadening of two-photon wave packets generated via type-I and type-II spontaneous parametric down-conversion," *J. Korean Phys. Soc.* **73**(11), 1650–1656 (2018).
21. B. Kozh, C. C. W. Lim, R. Houlmann, N. Gisin, M. J. Li, D. Nolan, B. Sanguinetti, R. Thew, and H. Zbinden, "Provably secure and practical quantum key distribution over 307 km of optical fibre," *Nat. Photonics* **9**(3), 163–168 (2015).
22. C. K. Hong, Z. Y. Ou, and L. Mandel, "Measurement of subpicosecond time intervals between two photons by interference," *Phys. Rev. Lett.* **59**(18), 2044–2046 (1987).
23. A. M. Steinberg, P. G. Kwiat, and R. Y. Chiao, "Dispersion cancellation in a measurement of the single-photon propagation velocity in glass," *Phys. Rev. Lett.* **68**(16), 2421–2424 (1992).
24. A. M. Steinberg, P. G. Kwiat, and R. Y. Chiao, "Dispersion cancellation and high-resolution time measurements in a fourth-order optical interferometer," *Phys. Rev. A* **45**(9), 6659–6665 (1992).
25. J. Perina Jr., A. V. Sergienko, B. M. Jost, B. E. A. Saleh, and M. C. Teich, "Dispersion in femtosecond entangled two-photon interference," *Phys. Rev. A* **59**(3), 2359–2368 (1999).
26. R. Erdmann, D. Branning, W. Grice, and I. A. Walmsley, "Restoring dispersion cancellation for entangled photons produced by ultrashort pulses," *Phys. Rev. A* **62**(5), 053810 (2000).
27. J. Ryu, K. Cho, C.-H. Oh, and H. Kang, "All-order dispersion cancellation and energy-time entangled state," *Opt. Express* **25**(2), 1360 (2017).
28. A. F. Abouraddy, M. B. Nasr, B. E. A. Saleh, A. V. Sergienko, and M. C. Teich, "Quantum-optical coherence tomography with dispersion cancellation," *Phys. Rev. A* **65**(5), 053817 (2002).
29. A. F. Abouraddy, M. B. Nasr, B. E. A. Saleh, A. V. Sergienko, and M. C. Teich, "Demonstration of dispersion-canceled quantum-optical coherence tomography," *Phys. Rev. Lett.* **91**(8), 083601 (2003).
30. V. Giovannetti, S. Lloyd, L. Maccone, and F. N. C. Wong, "Clock synchronization with dispersion cancellation," *Phys. Rev. Lett.* **87**(11), 117902 (2001).
31. J. D. Franson, "Nonlocal cancellation of dispersion," *Phys. Rev. A* **45**(5), 3126–3132 (1992).
32. S.-Y. Baek, Y.-W. Cho, and Y.-H. Kim, "Nonlocal dispersion cancellation using entangled photons," *Opt. Express* **17**(21), 19241 (2009).
33. I. C. Nodurft, S. U. Shringarpure, B. T. Kirby, T. B. Pittman, and J. D. Franson, "Nonlocal dispersion cancellation for three or more photons," *Phys. Rev. A* **102**(1), 013713 (2020).
34. H. de Riedmatten, I. Marcikic, W. Tittel, H. Zbinden, and N. Gisin, "Quantum interference with photon pairs created in spatially separated sources," *Phys. Rev. A* **67**(2), 022301 (2003).
35. S.-Y. Baek, O. Kwon, and Y.-H. Kim, "Temporal shaping of a heralded single-photon wave packet," *Phys. Rev. A* **77**(1), 013829 (2008).
36. H. F. Hofmann and S. Takeuchi, "Quantum phase gate for photonic qubits using only beam splitters and postselection," *Phys. Rev. A* **66**(2), 024308 (2002).
37. T. C. Ralph, N. K. Langford, T. B. Bell, and A. G. White, "Linear optical controlled-NOT gate in the coincidence basis," *Phys. Rev. A* **65**(6), 062324 (2002).
38. E. Knill, R. Laflamme, and G. J. Milburn, "A scheme for efficient quantum computation with linear optics," *Nature* **409**(6816), 46–52 (2001).
39. Y. Kim, K.-H. Hong, J. Huh, and Y.-H. Kim, "Experimental linear optical computing of the matrix permanent," *Phys. Rev. A* **99**(5), 052308 (2019).
40. M. Tillmann, B. Dakić, R. Heilmann, S. Nolte, A. Szameit, and P. Walther, "Experimental boson sampling," *Nat. Photonics* **7**(7), 540–544 (2013).
41. J. B. Spring, B. J. Metcalf, P. C. Humpherys, W. S. Kolthammer, X.-M. Jin, M. Barbieri, A. Datta, N. Thomas-Peter, N. K. Langford, D. Kundys, J. C. Gates, B. J. Smith, P. G. R. Smith, and I. A. Walmsley, "Boson sampling on a photonic chip," *Science* **339**(6121), 798–801 (2013).
42. Y. Kim, K.-H. Hong, Y.-H. Kim, and J. Huh, "Connection between BosonSampling with quantum and classical input states," *Opt. Express* **28**(5), 6929 (2020).

43. P. J. Mosley, J. S. Lundeen, B. J. Smith, P. Wasylczyk, A. B. U'Ren, C. Silberhorn, and I. A. Walmsley, "Heralded generation of ultrafast dingle photons in pure quantum states," *Phys. Rev. Lett.* **100**(13), 133601 (2008).
44. R. Kaltenbaek, B. Blauensteiner, M. Zukowski, M. Aspelmeyer, and A. Zeilinger, "Experimental interference of independent photons," *Phys. Rev. Lett.* **96**(24), 240502 (2006).
45. Y.-R. Fan, C.-Z. Yuan, R.-M. Zhang, S. Shen, P. Wu, H.-Q. Wang, H. Li, G.-W. Deng, H.-Z. Song, L.-X. You, Z. Wang, Y. Wang, G.-C. Guo, and Q. Zhou, "Dispersion effect on the single-photon wave-packet," arXiv:2007.10576.